Journal of Achievements in Materials and Manufacturing Engineering
VOLUME 17
ISSUE 1-2
July-August
2006

Effect of tool cutter immersion on Al-Si bi-metallic materials in High-Speed-Milling

J.H. Sokołowski [a], D. Szablewski [a, b, *], W. Kasprzak [a], E.G. Ng [c], M. Dumitrescu [c]
[a] Mechanical, Automotive, Materials Engineering, University of Windsor, 401 Sunset Ave., N9B 3P4, Windsor, ON, Canada
[b] Nemak of Canada Corporation, 4600 G.N. Booth Drive, N9C 4G8, Windsor, ON, Canada
[c] Materials Manufacturing Research Institute, McMaster University, 1280 Main St. West, L8S 4L7, Hamilton, ON, Canada
* Corresponding author: E-mail address: dszablew@nemak.com

Received 15.03.2006; accepted in revised form 30.04.2006

Manufacturing and processing

ABSTRACT

Purpose: Aluminum-Silicon (Al-Si) alloys are commonly used in the automotive industry. At high Si levels they offer good wear resistance. Abrasive wear however, has been identified as the main insert cutter damage mechanism during High-Speed-Milling (HSM). This study investigates the effect of the tool cutter immersion on Al-Si bi-metallic materials in HSM operation.
Design/methodology/approach: This study considers the effects of the tool cutter immersion on the resultant cutting forces, associated machined surface roughness, and machined subsurface microstructural damage caused by the tool cutter during the Minimum Quantity Lubricant – High Speed Milling (MQL-HSM) operation of Al-Si bi-metallic materials with varying amounts and morphologies of the silicon phase.
Findings: Experimental results indicate that a combination of gray cast iron with the W319 microstructure yields the greatest resistance to the tool cutter rake face during the face milling operation for all investigated tool cutter radial immersions. Machined surface roughness measurements reveal that surface roughness is a function of both the silicon content and morphology, as well as the percentage of tool cutter immersion. Matrix hardness measurements indicate that machining at all immersions has the same effect on compressing the matrix structure.
Research limitations/implications: This study considers the effects of the radial tooling immersion and material selection while the speed, feed, and axial depth-of-cut are kept constant. Future work should address variability in the machining parameters in an attempt to maximize tool life, while optimizing the machined surface quality.
Practical implications: Material selection affects the machining conditions in HSM of Al-Si bi-metallic materials. As a result careful consideration should be given when tailoring the machining conditions to the cast microstructures.
Originality/value: North American automakers rely heavily on Al-Si precision sand cast components. As a result bi-metallic machining has to be often addressed during the face milling of engine blocks and cylinder heads. The research conducted here broadens the understanding of the impact of radial immersion on the machining behavior of Al-Si bi-metallic materials.
Keywords: Machining; Al-Si alloys; Cutting forces; Subsurface damage

1. Introduction

Al-Si sand cast alloys are widely used due in part to their low specific gravity, low melting temperatures, high fluidity, and low shrinkage, which yields good castability and weldability, good corrosion resistance, and good thermal conductivity [1,2]. In the automotive industry Al-Si alloys are used to produce precision sand cast components using alloys 319.0, 355.0, A356, A357, and 443 with Si in the 5-7wt.% range. Die casting process allows the use of alloys with higher Si content. Si refinement in these castings is achieved mainly by rapid cooling rates. The Silicon in these cast components is in the 8-17% range, and alloy system designations are 380.0, 383.0, 384.0, 390.0, and 413.0 [1,2,5].

Irrespective of the Al-Si casting method the silicon morphology is controlled by the following factors: type and amount of modifier used (ex. Sr, Na, Sb), impurities present in the melt, alloy solidifying rate, and silicon content [1]. In general there are two types of silicon refinement: thermal (quench) modification, and chemical modification [1,6]. With the exception of the thin walled die castings, quench modification of silicon is impractical in industrial castings on a large scale due to the much slower cooling rates inherent to the industrial processes. Localized silicon morphological refinement in sand castings is possible, however, adjacent to the liner components in the engine blocks where liners act to some extent as chills refining the cast microstructure in the local zone surrounding the bores. These modified silicon structures can yield substantial improvements in machinability.

A study done on 380 cast components both unmodified and Na modified showed that unmodified structures yield much shorter tool life than modified structures do [7]. Another study of modification with cerium has shown to decrease the horsepower required to machine an Al-12%Si alloy, and to increase both the chip thickness ratio, and the shear plane angle [8]. However, literature concerning the effect of strontium modification on machinability is limited.

Machining of Aluminum-Silicon sand cast alloys is a unique fit for the novel High-Speed-Milling (HSM) technology. Relatively low melting points of a range of commercial Al-Si based alloys prevent the insert cutters from damage by thermal softening, and prevent diffusion damage [4]. High-Speed-Milling (HSM) of Al-Si cast alloys has been investigated to some extent. The melting point of pure aluminum is ~660°C, silicon and other alloy additions raise the liquidus of 3XX alloys up to ~720°C for alloys containing 20%Si. Tool cutters used to machine aluminum have melting points that are much higher than that temperature range. This allows high heat generation at the cutter rake face, which has a dual benefit allowing virtually unbound (in terms of the temperature) speeds to be used in machining aluminum alloys, while at the same time eliminating one of the main tool failure mechanisms – diffusion failure. The opportunity of increasing the cutting speed and feed improves throughput.

Machining bi-metallic materials at different tooling immersions offers challenges during Al-Si engine block manufacture. By selecting novel tool cutter materials and optimizing their geometry bi-metallic materials can be machined in a 'single-pass' operation. Variables such as speed, feed, axial and radial depths-of-cut, as well as the cutting environment (dry, flood coolant, or Minimum Quantity Lubricant - MQL) need to be optimized to tailor unique solutions to each machining operation.

Kishawy et al. [3] have investigated the effect of HSM of A356 cast alloy under flood coolant, dry, and Minimum Quantity Lubricant (MQL) conditions. They have found that MQL reduces the cutting forces at par with the flood coolant application up to a cutting speed of 4,000m/min for a sharp insert condition. In their study dry cutting resulted in the highest cutting forces for all cutting speeds. Insert cutter wear mechanism identified was mainly rake face abrasive wear, attributed to the sliding of the hard silicon phase particles over the tool rake face during the chip separation and evacuation.

This study considers the effects of the tool cutter radial immersion on the resultant cutting forces, associated machined surface roughness, and machined subsurface microstructural damage caused by the cutter during the Minimum Quantity Lubricant – High Speed Milling (MQL-HSM) operation of Al-Si bi-metallic materials with varying amounts and morphologies of the silicon phase.

2. Experimental procedure

2.1. Casting machining test blocks (MTB)

A Machinability Test Block (MTB) Zircon sand mold package was developed (see Figure 1). Three (3) types of hypereutectic Al-Si liners (15%SiESV, 15%SiREF, and 25%SiESV) developed independently as part of a Ph.D. dissertation [12] were incorporated into the MTB. The designation ESV refers to the modified Si structure, whereas REF refers to unmodified Si morphology. The liner microstructures have been modified using the novel liquid metal treatment method [13]. A gray cast iron liner was placed adjacent to each Al-Si liner type. In total three (3) MTB cast components were made. This mold design ensured reproducibility in each casting, and provided a relatively large volume to surface area ratio for the machining tests. Geometry of the MTB castings was determined to fit the dynamometric table, as indicated in Figure 2.

Table 1.
Chemistry of the W319 Al-Si alloy used in this study

Chemistry wt.%					
Si	Cu	Fe	Mg	Mn	Zn
7.47	3.68	0.39	0.25	0.25	0.18
Ti	Ni	Sn	Cr	Sr	Al
0.11	0.02	0.02	0.02	<.0005	bal.

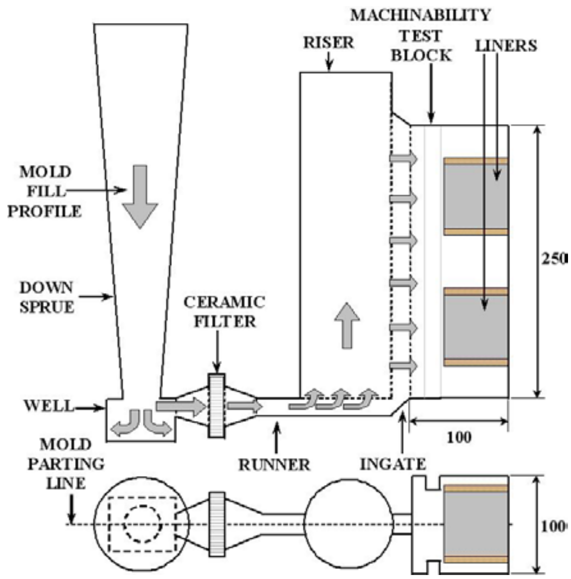

Fig. 1. A schematic diagram of the Machinability Test Block (MTB) casting mold showing the cross-sectional side view of the sand mold package along with the mold fill profile, and the cross-sectional top view of the mold package (MTB dimensions are in millimeters)

The casting alloy used was W319 (Table 1). The melt was degassed for 48 hours using a ceramic rod with a porous triangular head until the Reduced Pressure Test (RPT) reading gave an alloy density of 2.70grams/cm^3. Degassing gas used was N_2. The total weight of each MTB was 14.6+/-0.2kg (down sprue, well, runner, and riser included). This amount of alloy was hand-ladled into the molds using the industry-standard 30kg capacity steel ladle coated with mica. The alloy pouring temperature was 760°C. Mold filling time was 20.5+/-2.4s. Following complete casting solidification (below 300°C) the MTB castings were removed from the sand mold, and allowed to cool to ambient temperature. Risers and gating were then machined off, and the MTB were shot blast for 2 minutes to remove any excess Zr sand from the surface prior to machin

2.2. MTB machining & force measurements

Machining tests were performed using diamond coated carbide inserts in a Minimum Quantity Lubricant (MQL) environment, where the lubricant used was synthetic Phosphate Ester BM2000 with extreme pressure additives. The MQL was applied through an atomized spraying unit on the tool cutter at a rate of 10mL/h. Machining tests were carried out on a Makino MC56-5XA, 40HP, 15000-RPM, horizontal 5-axis milling machine. The face milling tool holder span used was 101.0mm. Two insert cutters were mounted on the tool holder opposite of each other (180° apart) in order to keep the tool balanced during operation. A spindle speed of 5000RPM was used (for a 101.0mm tool span this gave an approximate 3192m/min cutting speed), a feed of 0.2mm/tooth, and a 4.0mm axial depth-of-cut was used for all tests conditions.

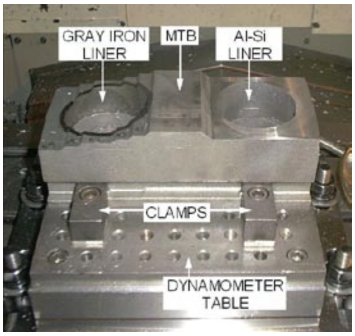

Fig. 2. Setup for the MTB HSM showing the MTB mounted on a Kistler 9255B type dynamometer table used for on-line cutting force measurements

The radial depth-of-cut varied from 25% (1/4 of the tool cutter span immersed in the microstructure during the cut), to 100% (the entire tool cutter immersed in the workpiece during face milling). Force acquisitions were made for each liner type at each immersion. The immersions used were 25, 40, 70, 85, and 100% (see Figure 3).

A Kistler 9255B, three component piezoelectric quartz crystal dynamometer table (see Figure 2) was used for on-line cutting force measurements. The x, y, and z force components were acquired for 3.0 seconds during the face milling while the tool cutter was immersed in the workpiece material to the target percentage of immersion. An average component value was then calculated. The x, y, z average force components were then used to calculate the average resultant force (F_R) acting on the tool cutter at each tool cutter immersion according to the equation:

$$F_R = \sqrt{\bar{x}^2 + \bar{y}^2 + \bar{z}^2} \qquad (1)$$

The resultant force was then plotted against the percentage of tooling immersion (see Figure 4). Following machining the MTB were dismounted from the dynamometer table, machined surface roughness measurements were then taken, and the MTB was sectioned for metallographic evaluation.

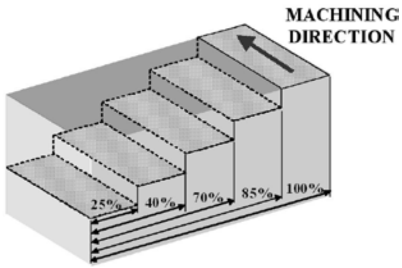

Fig. 3. A schematic representation of the tooling immersions used in this study

2.3. MTB surface roughness measurements

Machined surface roughness measurements were performed on the three (3) Al-Si liner types investigated at the five analyzed tool cutter immersions. The equipment used was a portable surface roughness gauge – FEDERAL POCKET SURF III. The standard measurement used was the arithmetic roughness (R_a) the units of which are microns [μm]. R_a is defined as the arithmetic average height of roughness irregularities measured from a mean line within the evaluation length [L]. The mathematical formula is:

$$R_a = \frac{1}{L}\int_0^L |y|dx \qquad (2)$$

where the evaluation length (L) used was 3.0mm. Ten (10) measurements were performed parallel to the machining direction, and perpendicular to the machining marks for each liner type, at each investigated tooling immersion. Average values and standard deviations were then evaluated (see Figure 5).

2.4. MTB metallographic sample preparation

The machined MTB were sectioned at each investigated tooling immersion. The cast W319, and the liner microstructures were then cold mounted. All samples were successively ground and polished using the BUEHLER grinding/polishing equipment. Grinding was done using the silicon carbide 240, 600, 800, and 1200 grit papers. The samples were then rough polished applying 1.0μm diamond suspension on a polishing cloth, and mirror polished using 0.5μm colloidal silica suspension.

2.5. MTB matrix hardness measurements

Vickers microhardness indentations were made using the CLEMEX 3.5 Automated Vickers Microhardness Tester. All indentations were made in the aluminum matrix using a load of 25 gram force (gf), applied for a duration of 15 seconds. Indentations were made at two distinct locations in each sample: directly below the machined surface (30µm from the machined surface), and inside the bulk liner structure (400µm from the machined surface). Ten (10) measurements were made at each conditions, averages and standard deviations where then calculated.

2.6. MTB light optical microscopy

A Leica 550 DMR Image Analysis system was used to quantify the primary silicon particle size in the three (3) liner types investigated at a magnification of X200. Leica QWin image analysis software was used to perform the thirty (30) individual measure-ements. Average and standard deviation values were then calculated.

2.7. MTB scanning electron microscopy

A JEOL – JSM 5800 Scanning Electron Microscope in the Secondary Electron mode (SEM/SE) was used to investigate the three (3) Al-Si liner type machined surfaces. Polished liner machining cross-sections were then investigated to asses the primary Si condition in the machined subsurface. All images were acquired at X600 magnification.

3. Results and discussion

3.1. Cutting forces

Measurements of the resultant cutting forces (F_R) during the face milling of the bi-metallic Al-Si sand-cast microstructures revealed that a combination of gray cast iron with W319 microstructure yields the greatest resistance to the tool cutter rake face during the face milling operation for all investigated tool cutter radial immersions (see Figure 4). The next highest F_R was observed in the 25%Si ESV liner combined with the W319 microstructure, this was followed by the 15% Si REF liner, and the 15%Si ESV liner offered the least resistance during the face milling operation. This is significant as it illustrates the relation between the size and morphology of the primary silicon phase and the resultant cutting force. The greater the primary particle size the higher the force exerted on the tool cutter during face milling. However, the results indicate that Al-Si liners, with Si as high as 25%, offer less resistance to the tool cutters than do the gray iron liners in the MQL-HSM operation at investigated machining conditions. At 25, 40, and 70% tooling immersions the 15%Si ESV liner which offered the least resistance to the tool cutters had an F_R of approximately 270N, the 15%Si REF liner had an F_R 22% higher at 333N, and the 25% Si ESV liner had an F_R 32% higher at 358N.

Tooling radial immersions of 25, 40, and 70% did not appreciably vary the F_R for any single investigated liner. The F_R for each machined casting/liner bi-metallic structure was within the standard deviation limits at these immersions. However, at 85 and 100% immersions, F_R was significantly higher over other tooling immer-sions. This increase in the F_R values is believed to be related to the volume of material the tool cutter is removing in each pass. Although tool wear rates were not measured in this study, it is reasonnable to conclude that they would be higher at 85 and 100% immersions.

3.2. Machined surface roughness

Machined surface roughness measurements of the three (3) investigated Al-Si liner types revealed that surface roughness is a function of both the silicon content and morphology, as well as the percentage of tool cutter immersion (see Figure 5). The shape of the graph closely mirrors the graph of the resultant cutting force (see Figure 4). The 25%Si ESV liner which had the highest amount of silicon, with the largest primary crystals, had the roughest machined surface at the 25, 40, and 70% tooling immersions. This was followed by the 15%Si REF liner, and then the 15%Si ESV liner. A maximum roughness for all three liner types occurred at 85% tooling immersion. The fact that the shape of the graph for the arithmetic surface roughness resembles the graph for the average resultant cutting force indicates that an increase in the cutting force degrades the machined surface finish.

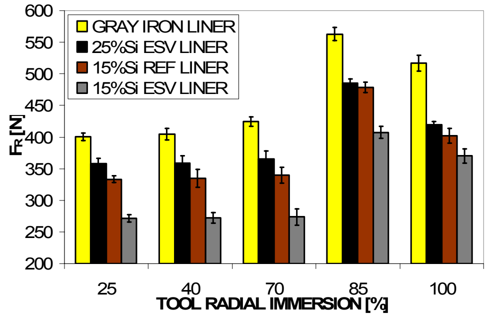

Fig. 4. Resultant cutting force (F_R) versus the percentage of the tool radial immersion for the three (3) Al-Si liner types investigated, as well as the gray iron liner commonly used in the industry. Standard deviations are as indicated

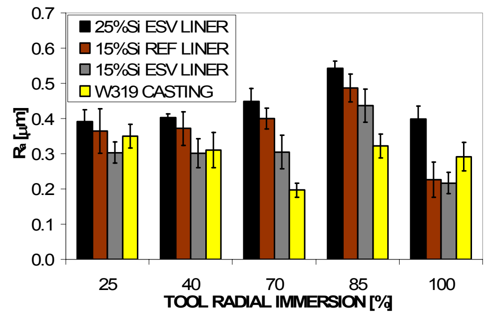

Fig. 5. Arithmetic average roughness (R_a) of the machined surface for the three (3) Al-Si liner types investigated, as well as the W319 machined surface, versus the percentage of the tool radial immersion. Standard deviations are as indicated

It is believed that the surface roughness is directly related to the size of the primary silicon crystals. The larger the size of the primary silicon particles in the relatively soft aluminum matrix structure, the lower the degree of microstructural homogeneity. As a result of this the response of the microstructure to the tool cutter rake face during the machining operation is non-uniform on the micro level. Since the material removal impacts the machined surface finish, the more inconsistent the material removal, the rougher the machined surface finish. Primary silicon particle fracture, and in some cases dislodging, illustrated in Figure 8 is direct evident of this.

3.3. Al-Si matrix hardness

Measurements of the matrix hardness in the immediate (30µm below) machined subsurface (see Figure 6a), and the bulk material (400µm below machined surface) matrix structure (see Figure 6b) indicate that machining at all tool immersions has the same effect of compressing the matrix structure. The subsurface matrix compresses the same amount independent of the tool immersion used. For the 25%Si ESV liner the HV25 was on average 12.2% higher in the subsurface than in the bulk matrix structure. In the 15%Si REF liner this number was 13.7%. In the 15%Si ESV liner it was 22.1%, and in the W319 casting it was 11.3%.

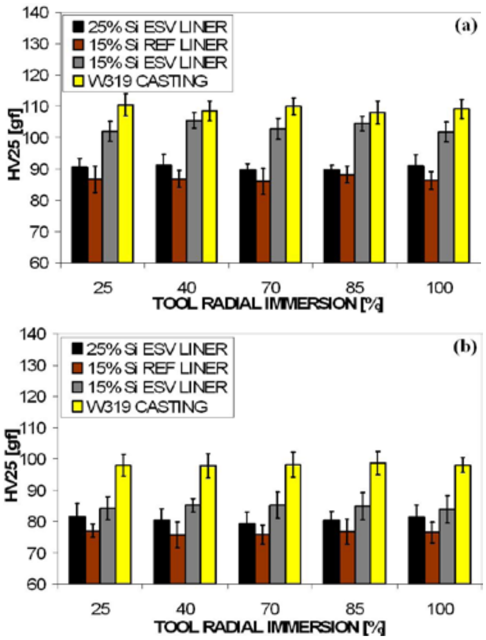

Fig. 6. Aluminum matrix microhardness (HV25) of the machined subsurface matrix structure (a), and the bulk material matrix structure (b) Al-Si cast liner structures for the three (3) investigated liner types, and the W319 cast matrix. Standard deviations are as indicated

3.4. Al-Si liner light optical microscopy

Light Optical Microscopy (LOM) investigation of the three (3) Al-Si liner types confirmed that the largest primary crystals exist in the 25%Si ESV liner, where the average dimensions were 112.0+/-5.6µm across. The 15%Si REF liner structure exhibited primary silicon with an average size of 76.2+/-4.3µm across. The 15%Si ESV liner on the other hand exhibited the smallest silicon particles, with an average primary Si size of 64.1+/-4.8µm across (see Figure 7).

3.5. Al-Si liner scanning electron microscopy

Scanning Electron Microscopy in the Secondary Electron Mode (SEM/SE) was performed on all Al-Si liner types. One liner type however, the 25%Si ESV liner, stood out from the rest of the liners due to its rough machined surface, and the presence of surface cavities (see Figure 8a). Close inspection of this machined surface revealed that the cavities were not formed during the casting process, which would have made them casting defects. Instead they were formed during the machining process. Close inspection of the inner walls of the cavities revealed that their surfaces were partially covered by the primary silicon phase. Analysis of the machined surface cross sections revealed the presence of multiple primary crystals with high density of fractures (see boxed regions in Figure 8b). All of the fractured crystals were located directly in contact with the machined surface suggesting that the tool cutter itself was the cause of this particle damage. A number of the fractured particle fragments appeared to have fallen out (see Figure 8b) creating the cavities observed on the machined surface in Figure 8a.

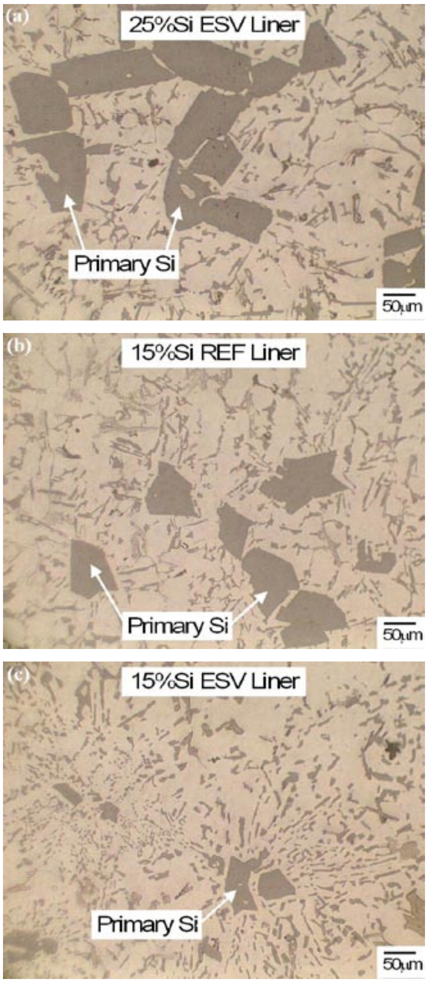

Fig. 7. Primary Si particle size comparisons between the three Al-Si liner types investigated

As can be imagined this mechanism of particle fracture, and in some cases fallout, is highly undesirable in the production process. It might resut in the least with poor surface finish, and may lead up to part damage. This is certainly the danger in the case of the machined liner inner surfaces where component sliding is a requirement of the part performance.

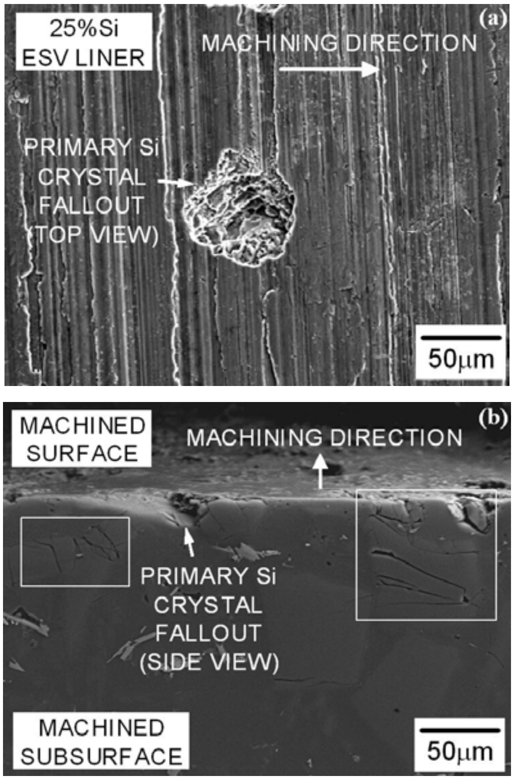

Fig. 8. SEM/SE micrographs of the 25%Si ESV liner machined surface showing two views: (a) top machined surface view, and (b) polished cross-sectioned side view

4. Conclusions

This study considered the effects of the radial tooling immersion during the High Speed Milling – Minimum Quantity Lubricant (HSM-MQL) of Al-Si sand cast bi-metallic microstructures at constant speed, feed, and axial depth-of-cut.

It was demonstrated that gray cast iron liners embedded in the W319 cast microstructure yield greater resistance to the tool cutter rake face during the HSM-MQL operation at tool cutter radial immersions ranging from 25 to 100% than do Al-Si liners with Si levels as high as 25wt.%.

Surface roughness assessment of the Al-Si liner machined surfaces reveal that given constant machining conditions used in this investigation surface roughness is a function of both the silicon content and morphology, as well as the percentage of tool cutter immersion. It was demonstrated that an increase in the resultant cutting force degrades the machined surface finish.

Matrix hardness measurements indicate that machining at all immersions has the same effect on compressing the matrix structure.

Scanning Electron Microscopy of the machined 25%Si ESV liner surface revealed that at such high Si concentrations the primary silicon particles tend to fracture heavily in the machined subsurface, which in some cases leads to particle fallout.

Future work should address variability in the machining parameters in an attempt to maximize tool life, while optimizing the machined surface quality.

Acknowledgements

This research is funded by AUTO21, a member of the Network of Centres of Excellence of Canada program. The authors would like to thank NEMAK of Canada for allowing the use of their facilities during the casting of MTB, and McMaster MMRI for machining of the test blocks. Special thanks to Dr. Francisco Carlos Robles Hernandez for providing the Al-Si liners.

References

[1] J.E. Gruzleski, B.M. Closset, The Treatment of Liquid Aluminum-Silicon Alloys, American Foudrymen's Society Inc., 1990.

[2] Information from http://www.Key-To-Metals.com, keyword: Aluminum-Silicon Alloys, August 27th, 2005.

[3] H.A. Kishawy, M. Dumitrescu, E.G. Ng, M.A. Elbestawi, Effect of coolant strategy on tool performance, chip morphology, and surface quality during high-speed machining of A356 aluminum alloy, International Journal of Machine Tools & Manufacture, v. 45, 2005, p. 219-227.

[4] M. Schultz, et al., Limits for the application of long protruding tools regarding the process stability and safety, Proceedings of the Second International Seminar on Improving Machine Tool Performance, La Baule, France, 2000.

[5] L. Backerud, G. Chai, J. Tamminen, Solidification Characteristics of Aluminium Alloys, v. 1-3, 1990.

[6] Lu Shu-Zu, A. Hellawell, The Mechanism of Silicon Modification in Aluminum-Silicon Alloys: Impurity Induced Twinning, Metallurgical Transactions, v. 18A, 1987, p. 1721-1733.

[7] C.A. Queener, W.L. Mitchell, Effect of Iron Content and Sodium Modification on the Machinability of Aluminum Alloy Die Castings, AFS Transactions, v. 73, 1965, p. 14-19.

[8] R. Sharan, N.P. Saksena, Rare Earth Additions As Modifiers of Aluminum Silicon Alloys, AFS International Cast Metals Journal, v. 3, 1987, p. 29-33.

[9] N. Tenekedjiev, H. Mulazimoglu, B. Closset, J. Gruzleski, Microstructures and Thermal Analysis of Strontium-Treated Aluminum-Silicon Alloys, American Foundrymen's Society Inc., 1995, p. 1-31.

[10] J.H. Sokolowski, M.B. Djurdjevic, C.A. Kierkus, Northwood D.O., Improvement of 319 Aluminum Alloy Casting Durability by High Temperature Solution Treatment, Journal of Materials Processing Technology, v. 109, 2001, p. 174-180.

[11] J.H. Sokolowski, X-C. Sun, G. Byczynski, D.O. Northwood, D.E. Penrod, R. Thomas, A. Esseltine, The Removal of Copper-Phase Segregation and the Subsequent Improvement in Mechanical Properties of Cast 319 Aluminum Alloys by a Two-Stage Solution Heat Treatment, Journal of Materials Processing Technology, vol. 53, 1995, p. 385-392.

[12] Francisco Carlos Robles Hernandez, Improvement in Functional Characteristics of Al-Si Cast Components through the Utilization of a Novel Electromagnetic Treatment of Liquid Melts, Ph.D. Dissertation, 2004, University of Windsor.

[13] Electromagnetic Method and Apparatus for Treatment of Engineering Materials, Products and Related Processes - IESV Technology Platform (US Provisional Patent Serial No. 60/431,236).